ELSEVIER

Chemical Engineering Journal 68 (1997) 103–114

Chemical Engineering Journal

Particle design
Part B: batch quasi-emulsion process and mechanism of grain formation of ketoprofen

F. Espitalier, B. Biscans, C. Laguérie

Laboratoire de Génie chimique, UMR CNRS 5503, ENSIGC, 18 Chemin de la Loge, 31078 Toulouse Cedex, France

Received 23 April 1996; revised 9 October 1996; accepted 7 April 1997

Abstract

This study deals with the spherical crystallization process by the quasi-emulsion mechanism, applied to a pharmaceutical. The objective is to produce spherical agglomerates made of a number of small crystals of the drug, having properties adequate for direct compression when manufacturing tablets. The aim of this work is to make the link between the process and these properties. The different steps occurring in the process are the formation of an emulsion whose droplets are made of the drug dissolved in a solvent, the creation of the supersaturation of the drug in the droplets by mass and heat transfer and the nucleation, growth and agglomeration of drug crystals inside the droplets.

The process has been carried out in a batch laboratory scale device. The variation of the operating parameters on the one hand and of the relative proportions of the various components on the other have enabled us to determine the influence on the internal and external structures of the produced agglomerates which influence the ability to be compressed. The identification of the phenomena occurring has led to a proposed mechanism for the formation of the agglomerates. © 1997 Elsevier Science S.A.

Keywords: Emulsion; Process; Spherical grains; Mass and thermal transfers; Crystallization

1. Introduction

In order to improve particle properties, new processes combining granulation and crystallization are being developed. This work deals with the spherical crystallization process by the quasi-emulsion mechanism applied to ketoprofen, a pharmaceutical drug [1]. This process allows production of spherical grains made of small crystals of a drug that have adequate properties for direct compression when manufacturing tablets [2,3].

The different steps occurring in the process are first the formation of an emulsion (the droplets are made of the drug dissolved in a good solvent and the continuous phase contains a poor solvent of drug and emulsifier), then the creation of the supersaturation of the drug into the droplets by mass and heat transfer, and finally the nucleation, the growth and the agglomeration of drug crystals inside the droplets [1].

PII S1385-8947(97)00057-0

2. Experimental apparatus and methods

2.1. Experimental apparatus

The experimental apparatus of the batch quasi-emulsion process is shown on Fig. 1. It is made up of four parts: a dissolution vessel (I), a transfer device (II), a crystallizer (III) and a pressurizing device (IV).

The dissolution vessel (I-1) is a reactor, 250 ml in volume, with an internal diameter of 60 mm in which the ketoprofen is dissolved in pure acetone. A cooler (I-5) prevents loss of acetone by evaporation. The crystallizer (III) is a 2.5 l capacity baffled vessel with an internal diameter of 150 mm. This vessel contains initially the aqueous solution. These two reactors have baffles (I-2 and III-2) and marine propellers (I-3 and III-3). The width of the baffles is equal to 1/10 the internal diameter of reactors. The diameter of the propellers has been chosen in order that the ratio D_p/D_r is between 0.4 and 0.6, so the propeller of the dissolution vessel has a diam-

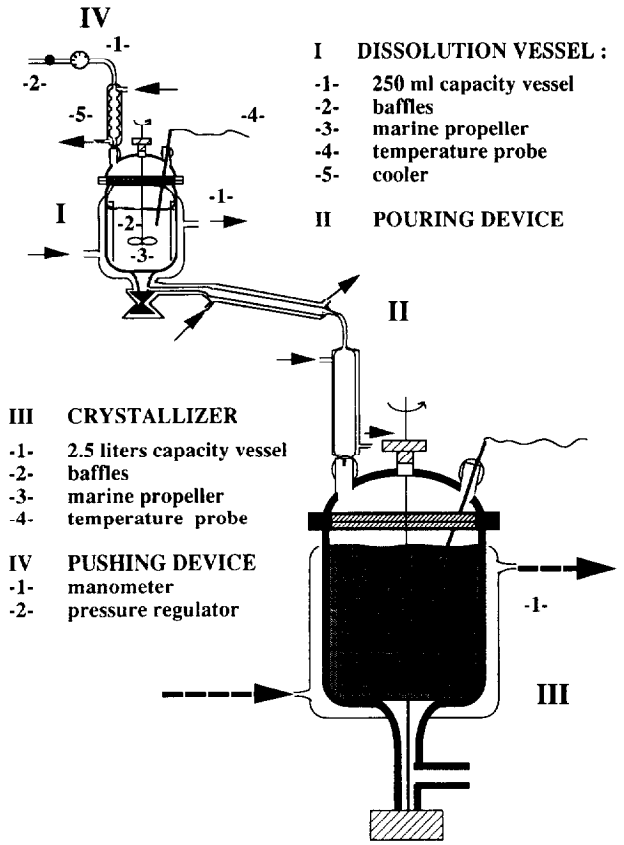

Fig. 1. Experimental apparatus of crystallization process by the quasi-emulsion process.

eter equal to 40 mm and the propeller of the crystallizer 60 mm.

The organic phase is poured into the aqueous phase by means of two devices: a pressurized device (IV) and a flowing down device (II) ended by a capillary with a variable diameter (1 or 2 mm). The organic solution trickles down in a regular flowrate. The temperatures of the dissolution reactor and of the flowing down device are controlled.

2.2. Operating conditions

For the experiment, first ketoprofen is dissolved in the dissolution reactor containing pure acetone at high temperature, T_1, which ranged between 48 and 50 °C. The dissolution time of ketoprofen is fixed at 2 h for all experiments. Then water containing a polyvinylic alcohol, mowiol 8–88 (0 to 500×10^{-6} kg mowiol kg^{-1} solution) is placed in a agitated crystallizer, and maintained at a temperature T_2 lower than T_1.

The relative proportion of ketoprofen/acetone has been chosen in accordance with the solubility curve of the ketoprofen in pure acetone. The boiling temperature of solution gives the maximum temperature T_1 while the difference of temperature (T_1-T_2) is changed in the process by modifying T_2.

The acetone + ketoprofen mixture is introduced at a constant flowrate into the aqueous solution. In the crystallizer, an emulsion is formed and in few minutes these droplets are transformed into spherical solid grains.

The system is thermally controlled at T_2 and the agitation of the system is maintained for at least 20 min. During this time, for a few experiments, sampling of suspension is carried out with a steel tube and a syringe, 50 ml in volume. These samples (1 to 2 ml) are immediately filtered with 0.45 μm filters and preserved in order to follow the concentration of acetone and ketoprofen in the continuous phase.

At the end of the experiment, the agglomerated crystals are recovered by filtration, washed with distilled water and dried in a drying oven at 50 °C for more than 24 h.

The operating parameters of the experiment are the flowrate of the ketoprofen + acetone solution, the stirring rate in the crystallizer, the difference of temperature (T_1-T_2), the diameter of capillary ending the pouring system and the residence time of the agglomerates in the crystallizer. The parameters characterizing the relative proportions of the compounds of the solutions are ketoprofen/acetone, acetone/water and mowiol/water ratios.

2.3. Analytical method

2.3.1. Solid characterization

The texture and the structure of grains obtained have been characterized by several techniques.

The flowability of grains is investigated by measuring the time, t_e, required for 100 g of grains to flow through a calibrated funnel. The flow has been recorded by a video camera in order to analyse the flow consistency. From the video film, the volume of grains falling in the graduated test tube is noted as a function of time.

Before this flow test, grains are divided twice into eight statistically equal samples by a RESCHT divider to measure their size and to observe their structures.

The median size and size distribution of a sample is measured by a laser sizer GALAI CIS-1. The grains are suspended in distilled water in the cell of a laser sizer with a peristaltic pump for 5 min. Water is a non-solvent [1] and improves the dispersion of agglomerated grains. The mass of grains used is about 2 g. The GALAI system of analysis gives access to statistical data. These statistical data, for example, are the size distribution in number, surface and volume. In this work, the results are presented in terms of volume. The mean diameter, $\bar{d}_v$, and the standard deviation, σ_d, are respectively given by the following equations:

$$\bar{d}_v=\frac{\Sigma(\bar{d}_n)_i^4 dn_i}{\Sigma(\bar{d}_n)_i^3 dn_i} \quad (1)$$

$$\sigma_d=\left(\frac{\Sigma(\bar{d}_n-\bar{d}_v)^2\bar{d}_{n_i}^3 dn_i}{\Sigma\bar{d}_{n_i}^3 dn_i}\right)^{1/2} \quad (2)$$

where dn_i is the number percentage of particles with a mean diameter in class i equal to $(\bar{d}_n)_i$.

The median diameter corresponds to the size at which the cumulative distribution curve equals 50%. The particles with

Table 1
Size of grains before and after the tapping tests

	Size data	
	Before the tests	After the tests
Mean diameter (μm)	259	215
Standard deviation (μm)	181	163
Median diameter (μm)	198	162
Fine particles (%)	10.66	18.07
Coarse particles (%)	9.98	6.13

a size smaller than 100 μm have here been called fine and those with a size greater than 500 μm are called coarse particles. The median diameter, the mean diameter, the standard deviation and the percentages of fine and coarse particles will be given as results of the distribution for each experiment.

In order to observe the shape, the surface topographies and the internal structures of grains we have used a scanning electronic microscope (SEM).

The apparent densities have been obtained by means of a Hosokawa powder analyser. A mass of grains corresponding to 100 cm^3 in volume has been measured, before and after 10, 100, 200, 400 and 500 tappings; 500 are necessary to obtained the tapped apparent density. The apparent density, ρ_{app}, and tapped apparent density, ρ'_{app}, are given by the equations

$$\rho_{app} = \frac{m_0}{100} \quad (g\ cm^{-3}) \tag{3}$$

$$\rho_{app}' = \frac{3}{\left(\frac{100}{m_0} + \frac{200}{m_{500}}\right)} \quad (g\ cm^{-3}) \tag{4}$$

where m_0 is the initial mass and m_{500} is the mass after 500 tappings.

2.3.2. Liquid analysis

During the experiments, in order to investigate the diffusion process of acetone and ketoprofen, concentrations of those products are regularly measured in the continuous phase by high performance liquid chromatography. During the first seconds of the experiment, it is very difficult to separate the dispersed phase from the continuous phase: the droplets go through the filter and so the concentrations of acetone and ketoprofen in the continuous phase cannot be obtained.

3. Preliminary experiments

3.1. Strength of grains

During the analysis, the grains can be submitted to stresses modifying their size and shape. To analyse these stresses, tests of fragility have been carried out. Measurements of mean and median diameters and standard deviation against the circulation time in the peristaltic pump used in size analysis have shown that the pump does not break the grains. In Table 1, size distributions of grains, before and after tapping tests, are reported for a standard experiment. The size distribution is shifted to smaller values.

3.2. Experiment reproducibility

Crystallization process reproducibility has been tested. Table 2 summarizes the operating conditions of these experiments. It can be seen that there are small differences of pouring flowrates and of mowiol concentration between these experiments. The results of these experiments, reported in the same table, show good reproducibility. The apparent densities and the tapped apparent densities are the same and the concentrations of acetone in mother liquors are quasi-equal: ±7% from the mean value. On the other hand, the concentrations of ketoprofen do not seem reproducible. This heter-

Table 2
Operating conditions and results of experiments of reproducibility

	Experiments		
	1	2	3
Operating conditions			
Stirring rate (rpm)	500	500	500
Diameter of phial (m)	0.002	0.002	0.002
ΔT (°C)	29.1	29	29
Pouring rate × 10^6 ($m^3\ s^{-1}$)	7.8	7.2	6.9
$W_k \times 10^6$ (kg ketoprofen/kg suspension)	0.042	0.042	0.042
$W_m \times 10^6$ (kg mowiol/kg suspension)	215	224	215
W_a (kg acetone/kg suspension)	0.022	0.023	0.022
Analysis of liquid filtrated			
W'_a (kg acetone/kg solution)	0.022	0.024	0.025
$W'_k \times 10^6$ (kg ketoprofen/kg solution)	432	228	367
Analysis of solid: apparent densities ($g\ cm^{-3}$)			
Apparent density	0.47	0.47	0.47
Tapped apparent density	0.51	0.52	0.52
After 10 tappings	0.49	0.50	0.50
After 100 tappings	0.51	0.52	0.52
After 200 tappings	0.52	0.53	0.53
After 400 tappings	0.53	0.54	0.54
After 500 tappings	0.54	0.54	0.54
Size data before the tapping tests			
Mean diameter (μm)	251	257	268
Standard deviation (μm)	180	178	198
Median diameter (μm)	182	187	188
Fine particles (%)	11.92	14.17	13.9
Coarse particles (%)	9.93	10.04	12.8
Mass balance on solid			
Initial mass of ketoprofen (g)	90.78	90.92	90.59
Final mass of grains (g)	87.33	87.22	87.20
Loss during filtration (g)	0.84	0.44	0.72
Mass balance (%)	−2.9	−3.6	−2.9

Table 3
Operating conditions of experiments

Experiment no.	W_k (kg ketoprofen/kg acetone)	$W_m \times 10^6$ (kg mowiol/kg water)	W_a (kg acetone/kg water)	ΔT (°C)	$Q_c \times 10^6$ ($m^3 s^{-1}$)	N (rpm)	d_c (m)	Dissipated power $P_s^* \times 10^2$ (W/kg suspension)
1	1.92	230	0.024	29.1	7.8	516	0.002	8.7
2	1.93	240	0.025	29	7.2	516	0.002	8.7
3	1.92	230	0.024	29	6.9	516	0.002	8.7
4	1.92	220	0.024	28.9	0.31	516	0.001	8.7
5	1.93	230	0.023	29.2	0.94	516	0.001	8.7
6	1.91	232	0.024	28.4	2.0	516	0.001	8.7
7	1.95	230	0.024	29.5	2.0	516	0.001	8.7
8	1.91	230	0.024	28.3	2.4	516	0.001	8.7
9	1.92	228	0.024	29	6.1	516	0.001	8.7
10	1.94	229	0.023	9.4	2.4	516	0.001	8.7
11	1.98	224	0.023	13.9	2.3	516	0.001	8.7
12	1.93	230	0.024	18.9	2.4	516	0.001	8.7
13	1.93	230	0.024	39.5	2.2	516	0.001	8.7
14	1.93	230	0.024	28.9	2.4	664	0.001	18.7
15	1.93	232	0.024	40	1.3	516	0.001	8.7
16	1.93	243	0.04	29.2	2.5	516	0.001	8.4
17	1.94	225	0.055	28.8	2.3	516	0.001	10.7
18	1.94	218	0.078	28.9	2.3	516	0.001	7.2
19	1.94	966	0.023	29.2	0.94	516	0.001	8.7
20	0.98	253	0.025	27.7	3.5	516	0.001	8.9
21	1.93	225	0.055	27.1	2.9	516	0.001	10.7
22	1.96	161	0.023	0.9	1.5	516	0.001	8.7
23	1.73	223	0.026	29.4	1.3	516	0.001	8.7
24	1.88	227	0.024	38.4	2.2	516	0.001	8.7
25	1.94	225	0.054	27.1	3.0	450	0.001	7.3
26	1.92	225	0.078	27.7	2.7	416	0.001	8.7
27	1.91	512	0.023	26.2	3.0	516	0.001	8.7
28	1.01	239	0.028	27.7	3.5	516	0.001	8.9
29	1.91	0	0.024	28.3	2.4	516	0.001	8.7
30	1.79	237	0.025	30.4	1.89	516	0.001	8.7
31	1.94	227	0.055	28.5	1.89	516	0.001	10.7

ogeneity could be developed during filtration or during sampling of the solution or from a very quick evolution of sample concentration with time. However, the absence of reproducibility of ketoprofen concentrations must be minimized because these concentrations are lower than 2000 ppm. The error made during the quantity determination is lower than 1%.

The diameters of grains are reproducible about 2 to 4% around the mean value. Finally, the reproducibility of process experiments based on size distribution can be considered as satisfactory.

4. Experimental results

The operating conditions of the different experiments are summarized in Table 3. Experiments are carried out over 20 min because the composition of the continuous phase becomes almost constant after this period. Two experiments have required more time (experiments 10 and 22). Experiments at different stirring rates have determined an operating range. The minimal stirring rate equal to 402 rpm corresponds to the stirring rate under which spherical grains adhere to each other in the crystallizer after 20 min. The upper limit (664 rpm) is fixed by the design of the equipment.

4.1. Solvent transfer

The transfer of solvents is influenced by several factors. The influence of the following parameters on the mass transfer of acetone are discussed here: the initial temperature T_2 and the acetone/water, mowiol/water and ketoprofen/acetone ratios.

In order to investigate the contribution of temperature, T_1 has been maintained at a constant value as T_2 has been varied. Experiments have been carried out with three different temperatures T_2. The results are shown in Fig. 2(a) and (b). The final mass fraction of acetone in the continuous phase increases by increasing the temperature and tends towards a maximum equal to $W_a/(1+W_a)$. A low difference of initial temperatures between the two phases accelerates the mass transfer of acetone outside the droplets. However, we have observed that this low difference leads to an agglomeration of grains in the crystallizer. Fig. 2(b) shows that the mass fraction of ketoprofen reaches a maximum and then decreases down to a quasi-constant mass fraction. For the experiment

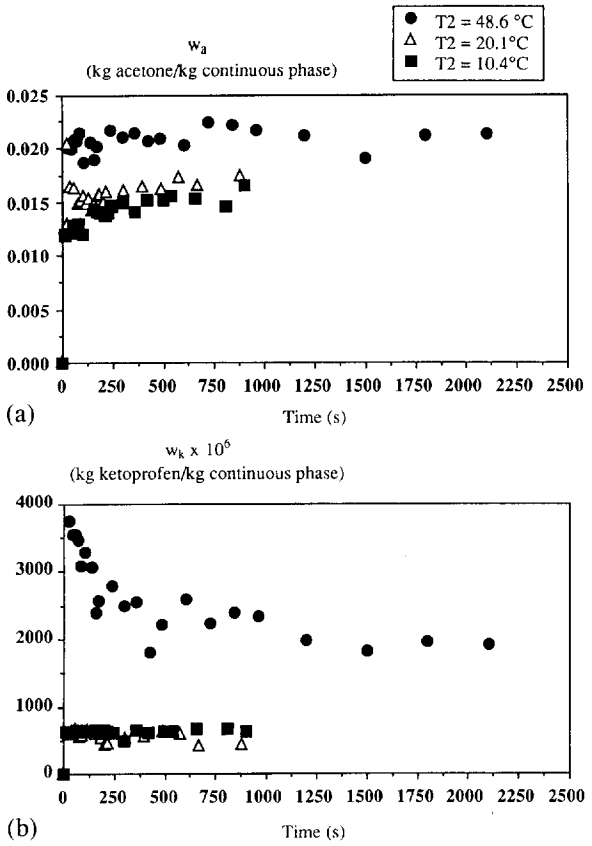

Fig. 2. Evolution of mass fractions in continuous phase in accordance with initial temperature T_2 of (a) acetone; (b) ketoprofen.

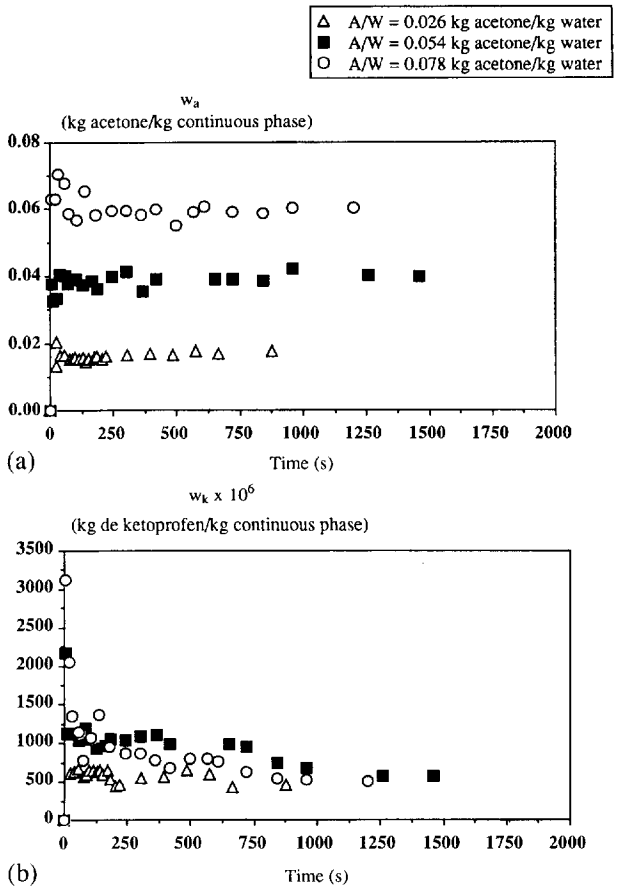

Fig. 3. Evolution of mass fractions in continuous phase in accordance with initial mass ratio of acetone/water of (a) acetone; (b) ketoprofen.

with a temperature T_2 of 48.6 °C, the maximum mass fraction reaches 3733 ppm. In that case, it can be assumed that an excess of ketoprofen is carried out by a strong flux of organic phase. Then, ketoprofen crystallizes and the formed crystals stick on the grains, leading to a decrease of mass fraction of dissolved ketoprofen in the continuous phase.

Experiments have been carried out with three different mass ratios, 0.026, 0.054 and 0.078 kg acetone/kg water. Fig. 3(a) and (b) show respectively the influence of this parameter on the mass fraction of acetone and of ketoprofen in the continuous phase. The maximum mass fraction of acetone increases when the initial ratio increases (Fig. 3(a)). According to Fig. 3(b), the initial value of ketoprofen mass fraction increases when the ratio of acetone/water increases. But the initial ratio of acetone/water does not influence the final mass fraction of ketoprofen in the continuous phase. This mass fraction is constant and equal to 505 ± 52 ppm.

Two ratios of mowiol/water have been studied, 223×10^{-6} and 512×10^{-6} kg mowiol/kg water. The final mass fractions of acetone and ketoprofen in solution are not influenced by the ratio of mowiol/water. In the same way, the evolution of the mass fraction of acetone in the continuous phase is not influenced by the ratio of ketoprofen/acetone.

According to our results two basic parameters influence this transfer: the difference of temperatures $(T_1 - T_2)$ and the initial mass ratio (acetone/water).

4.2. Grain properties

4.2.1. Apparent densities

The apparent densities of agglomerates depend on the flowrate at which the ketoprofen solution was poured. Apparent density and tapped apparent density, for experiments 4 to 9, decrease when the flowrate increases. For flowrates higher than 2.4 $cm^3\ s^{-1}$, the apparent density and tapped apparent density remain constant and respectively equal to 0.47 and 0.50 g cm^{-3}. However, a flowrate lower than 0.3 $cm^3\ s^{-1}$ permits us to obtain an apparent density equal to 0.53 g cm^{-3} and a tapped apparent density equal to 0.61 g cm^{-3}. These two values are interesting to give adequate properties of comprimability to the drug. The evolution of apparent densities in accordance with tapping number and different flowrate values has been studied. We have noted that the densities increase sharply from the first 10 tappings. Then the apparent densities continue to increase more slowly. These densities remain constant after 200 tappings.

From results corresponding to experiments 8, 10, 11, 12 and 13, the difference of temperature $(\Delta T = T_1 - T_2)$ does not have a significant effect on the apparent densities. When ΔT is small (for $\Delta T = 10$ °C and smaller values) agglomeration of grains has been observed in the crystallizer. This agglomeration begins after about 20 min. For higher ΔT

(=40 °C), the required residence time is higher than 20 min: grains need 60 min to solidify. An experiment with ΔT equal to zero has been done. The grains formed are agglomerated and need 35 min to solidify. The results concerning the influence of tapping number on apparent densities are identical to results observed during the study of the influence of flowrate.

Two stirring rates have been studied: 516 and 664 rpm. In the presented results, the dissipated power and the rate of breaking the pouring jet vary from one experiment to another. The dissipated powers are given in Table 3. The apparent densities are not modified by agitation.

Two diameters of pouring capillary have been used: 1 and 2 mm (experiments 1 and 6). The study has been made with a constant linear rate. This diameter has no influence on apparent densities.

Fig. 4 shows the influence of the relative proportions of acetone/water on the apparent densities for experiments 8, 16, 17 and 18. The variation of this ratio involves the variation of the suspension volume into the crystallizer. In practice, to increase the ratio of acetone/water, the mass of water has to be decreased because of the limited capacity of the dissolution reactor. Therefore, the dissipated power is modified even if the stirring rate is kept constant. Identical stirring rates lead to the same break of jet. Points 1, 2 and 3 on Fig. 4 correspond to the same stirring rate (516 rpm), and points 1, 2 and 4 are made for the same dissipated power. At constant dissipated power, the apparent densities decrease when the ratio of acetone/water increases. But for constant stirring rate, the ratio of acetone/water has no influence on the apparent densities.

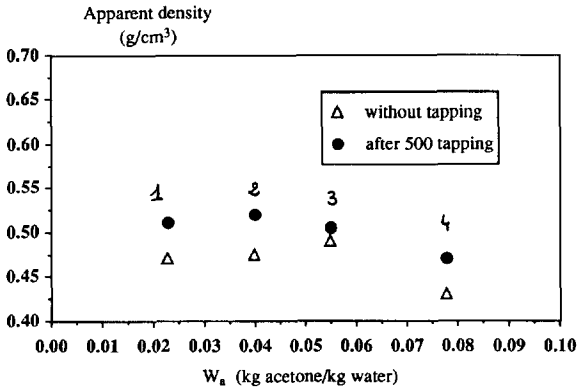

Fig. 4. Influence of initial mass ratio of acetone/water on apparent density and tapped apparent density.

The Carr index is equal to the relative difference between the apparent tapped density and the apparent density. Fig. 4 shows that these two apparent densities are quasi-equal for a mass ratio equal to 0.055 kg acetone/kg water. So, for identical stirring rates, but with different dissipated powers, the Carr index decreases. The decrease of this index leads to a better flowability of grains.

Three relative proportions of mowiol/water have been studied: 0, 230×10^{-6} and 960×10^{-6} kg mowiol/kg water (experiments 5, 19 and 29). These experiments have shown that an emulsifier is necessary to form the droplets (experiment 29) and for high mowiol/water a coalescence of grains is observed (experiment 19). This agglomeration leads to an important loss of product during filtration. Apparent density

Table 4
Influence of flowrate on distribution size

No.	Flowrate $\times 10^6$ ($m^3 s^{-1}$)	Mean diameter (μm)	Standard deviation (μm)	Median diameter (μm)	Percentage lower than 100 μm	Percentage higher than 500 μm
Before 500 tappings						
15	1.3	260	184	199	11.30	9.90
13	2.2	237	171	179	11.62	7.67
After 500 tappings						
4	0.31	240	184	174	23.92	9.17
5	0.94	223	179	156	23.89	7.96
6	2.0	214	167	153	21.51	7.11
7	2.0	217	174	150	24.94	7.58
8	2.4	233	183	166	25.94	8.38
9	6.1	224	177	165	24.38	7.32

Table 5
Influence of temperature difference ΔT on distribution size

No.	ΔT (°C)	Mean diameter (μm)	Standard deviation (μm)	Median diameter (μm)	Percentage lower than 100 μm	Percentage higher than 500 μm
Before 500 tappings						
10	9.4	291	175	262	8.49	10.92
11	13.9	255	189	185	12.29	10.73
12	18.9	252	188	189	15.18	10.17
8	28.3	233	184	165	26.45	4.74
After 500 tappings						
13	39.5	237	171	179	11.62	7.67

sharply increases when the relative proportion of mowiol/water decreases.

4.2.2. Size distribution

The results of size analysis are reported in Table 4. The size analysis shows that the median diameter and the percentage of coarse grains decrease when the flowrate increases and the percentage of fine particles is quasi-constant. However after the tapping tests, the size distributions are the same for all flowrates.

Table 5 gives the results of size analysis as function of ΔT. When ΔT increases, the median diameter and the percentage of fine particles decrease.

The median diameter is reduced and the percentage of fine particles enlarges when the stirring rate increases (from 26% for 516 rpm to 31% for 664 rpm). The mean diameter of grains increases from 220 to 270 μm when the diameter of the capillary increases.

Experiments 8, 16, 17 and 18, reported in Table 6, show that an increase of the acetone/water ratio causes an increase of the median diameter (234 μm for experiment 17 and 474 μm for experiment 18) and an increase in the number of coarse particles. The percentage of fine particles increases when the acetone/water ratio decreases.

Median diameter and percentage of coarse particles are enlarged by an increase of relative proportion of mowiol/water (because of the agglomeration phenomenon).

The percentage of fine particles is high (between 19 and 25%). When the ketoprofen ratio decreases (for experiments 8 and 20), the percentage of fine particles seems to decrease.

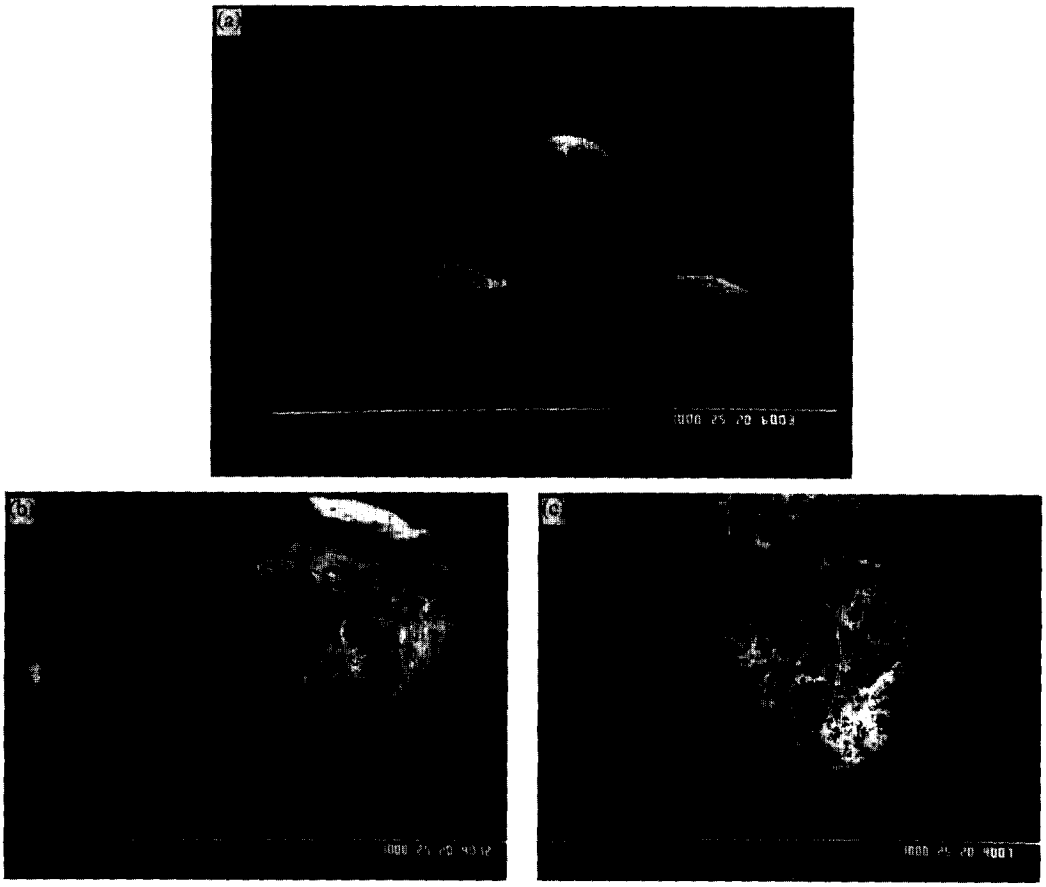

Fig. 5. Grains obtained by the quasi-emulsion process: (a) spherical grain; (b) non-spherical grain (experiment 18); (c) deformed sphere (experiment 10).

Table 6
Influence of initial acetone/water ratio on size data

No.	Acetone/water ratio (kg acetone/kg water)	Mean diameter (μm)	Standard deviation (μm)	Median diameter (μm)	Percentage lower than 100 μm	Percentage higher than 500 μm
Before tapping						
18	0.078	486	211	474	1.93	42.81
17	0.055	278	162	234	4.81	7.55
After tapping						
18	0.055	267	159	220	5.42	7.19
16	0.040	245	186	177	16.68	10.24
8	0.023	233	183	165	25.94	8.38

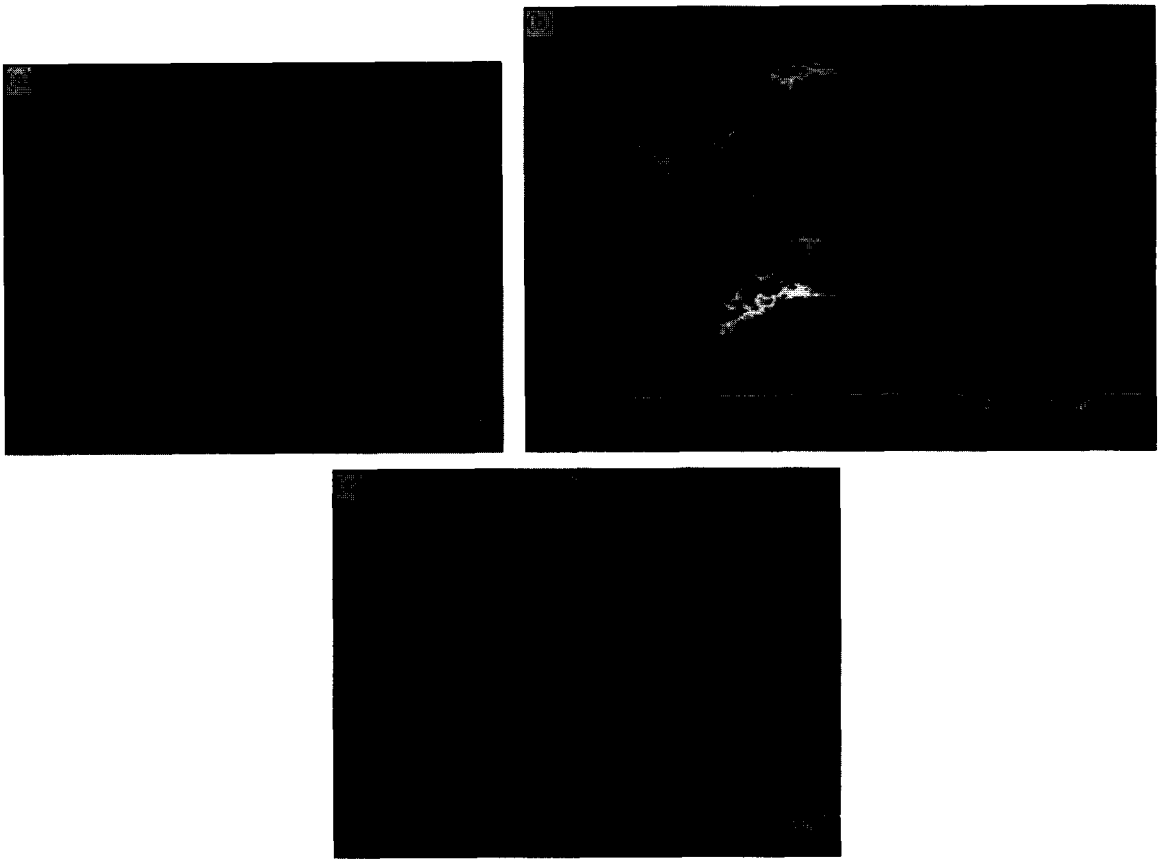

Fig. 6. Coalescence and agglomeration during the process: (a) coalescence of droplets leading to a deformed grain (ΔT=9.4 °C, experiment 10); (b) agglomeration of grains (966 ppm mowiol, experiment 19); (c) deformed grain (966 ppm mowiol, experiment 19).

4.2.3. Flowability

All samples have flow time ranged between 7.5 and 13 s. Only two experiments lead to a flow time higher than 15 s (experiments 19 and 11). These results have been compared to results obtained with glass balls with a mean diameter equal to 250 μm. In that case, the flow time is equal to 3 s. So the flowability of grains is good while their flow times are higher than those of glass balls. Properties of the product can explain this difference. The study of flow by camera has shown that the flow is not regular.

5. Grain structure

SEM photographs of the agglomerated crystals of ketoprofen have shown that two shapes of agglomerates and two internal structures can be found.

5.1. External structure

Spherical grains (Fig. 5(a), experiment 13) and non-spherical grains (Fig. 5(b), experiment 18) are obtained. Among non-spherical grains, some are elongated (Fig. 5(b)) and some are deformed spheres (Fig. 5(c)). Three parameters have an influence on the form of the grains: difference of initial temperature, initial concentration of mowiol and initial ratio of acetone/water.

The sphericity of grains decreases when the acetone/water ratio increases. For a ratio higher than 0.060 kg acetone/kg water, we have systematically found elongated grains. The difference of temperature and the concentration of mowiol can lead to coalescence of droplets or to agglomeration of grains in the crystallizer. Fig. 6(a) (experiment 10, ΔT=9.4 °C) and Fig. 6(b) (experiment 19: 966 ppm mowiol) show respectively the coalescence of droplets before the crystallization and agglomeration of grains. Fig. 6(c) displays the distortion of droplets during the process due to an high concentration of mowiol (experiment 19). The grains in Fig. 6(b) have an external surface rougher than those obtained with lower concentration of mowiol (Fig. 7(a), experiment 4). The difference of temperature also seems to have an effect on the surface of grains. Fig. 7(a) (ΔT<35 °C) and Fig. 7(b) (ΔT>35 °C, experiment 13) exhibit different surface states. For ΔT lower than 35 °C, the faces of crystals on the surface are perceptible (Fig. 7(a)), and for ΔT higher than 35 °C, developed faces are oblique and disorganized (Fig. 7(b)). The mechanism of grain formation varies as a function of ΔT.

Moreover, several holes randomly scattered over the surface of all the agglomerates have been observed. Two explanations can be given:

- these holes may be created by impacts (impacts of agglomerates/stirrer, impacts of agglomerates/baffles)

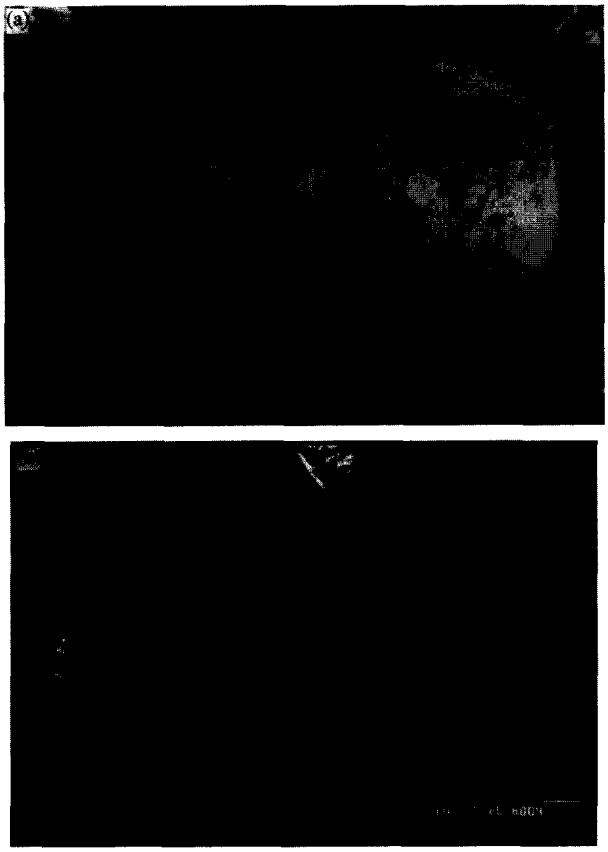

Fig. 7. Surface and oriented crystal faces: (a) the faces most developed are visible ($\Delta T < 35$ °C, experiment 4); (b) the developed faces are oblique ($\Delta T > 35$ °C, experiment 13).

- interfacial movements caused by opposite mass transfers of two solvents can create brutal jets of solvents that run through the interfacial crust [4].

5.2. Internal structure

A cut made on grains has permitted us to observe internal structures. Two types of internal structure exist:

- hollow spherical agglomerates (see Fig. 8(a))
- full spherical agglomerates (see Fig. 8(b)).

The hollow grains have a dense crust in which the crystals seem to have two orientations. On the edge of the grain, the longest faces of the crystals are perpendicular to the radius of the grain. These crystals form the first crust. From this first crust, other crystals are developed: their longest faces are now parallel to the radius of the grain (see Fig. 8(c)). These crystals form the second crust.

The internal structure depends essentially on the difference of temperatures between the two phases and on the initial ratio of acetone/water. In the hollow grains, the thickness of the crust surrounding the grains is a function of the difference of temperature ($T_1 - T_2$). When this difference decreases, the thickness of the crust increases and this crust becomes more dense. So we can suppose that only one crust is formed for ΔT higher than 35 °C. The single presence of the second crust explains the difference of external surface for ΔT higher than 35 °C. Fig. 8(a), (b) and (d) illustrate the influence of ratio of acetone/water on the internal structures for ratios equal respectively to 0.023, 0.052 and 0.078 kg acetone/kg water. In this case, the crust observed occupies all the grain and becomes dense when the initial ratio increases. These differences of internal structures explain the low Carr index obtained for the initial ratio equal to 0.055 kg acetone/kg water (see Section 4.2.1, Fig. 4). Full grains are formed when the initial ratio becomes higher than 0.05 kg acetone/kg water. The other grains have a hollow structure.

6. Mechanism of formation of grains

The different structures obtained by varying the two main operating parameters (difference of initial temperature and acetone/water ratio) are illustrated by Fig. 9. Three steps must be taken into account to explain the formation of the grains: formation of droplets, creation of supersaturation and crystallization of ketoprofen into droplets. When the droplets are formed, three phenomena are in competition: mass transfer, heat transfer and internal hydrodynamic circulation.

6.1. Size of droplets

The initial size of droplets influences the importance of the previously cited phenomena. The size of droplets depends essentially on the flowrate of the organic solution, on the diameter of the falling jet, on the proportion of mowiol in water and on the stirring rate. The size of droplets induces the different internal structures observed: those with one crust, with two crusts, and full internal structure. The mechanism of formation is summarized in Fig. 10. The various steps described are explained below.

6.2. Creation of supersaturation

The heat and mass transfers lead the droplet to a supersaturation state allowing crystallization. This has been studied separately from equilibria data. Here, we divide the droplet into different concentric layers in order to analyse the supersaturation in the droplet. The supersaturation ratio in a layer j is called S^j. The layers are numbered from the solid/liquid interface.

Determination of equilibrium data of the ketoprofen/acetone/water system has shown that the solubility of ketoprofen increases in the acetone + water solvent as the temperature increases [5]. So, the temperature of hot droplets formed in the cold continuous phase decreases from the interface to the centre. The droplet develops a higher supersaturation ratio at its surface than in its centre ($S^1 > S^2 > S^3 > S^4 > S^5 \ldots$). Therefore, by creating a difference of temperature ($T_1 - T_2$), the crystals of ketoprofen appear preferentially at the interface.

Moreover, for the ternary system, ketoprofen/acetone/water, at constant temperature, the solubility of ketoprofen

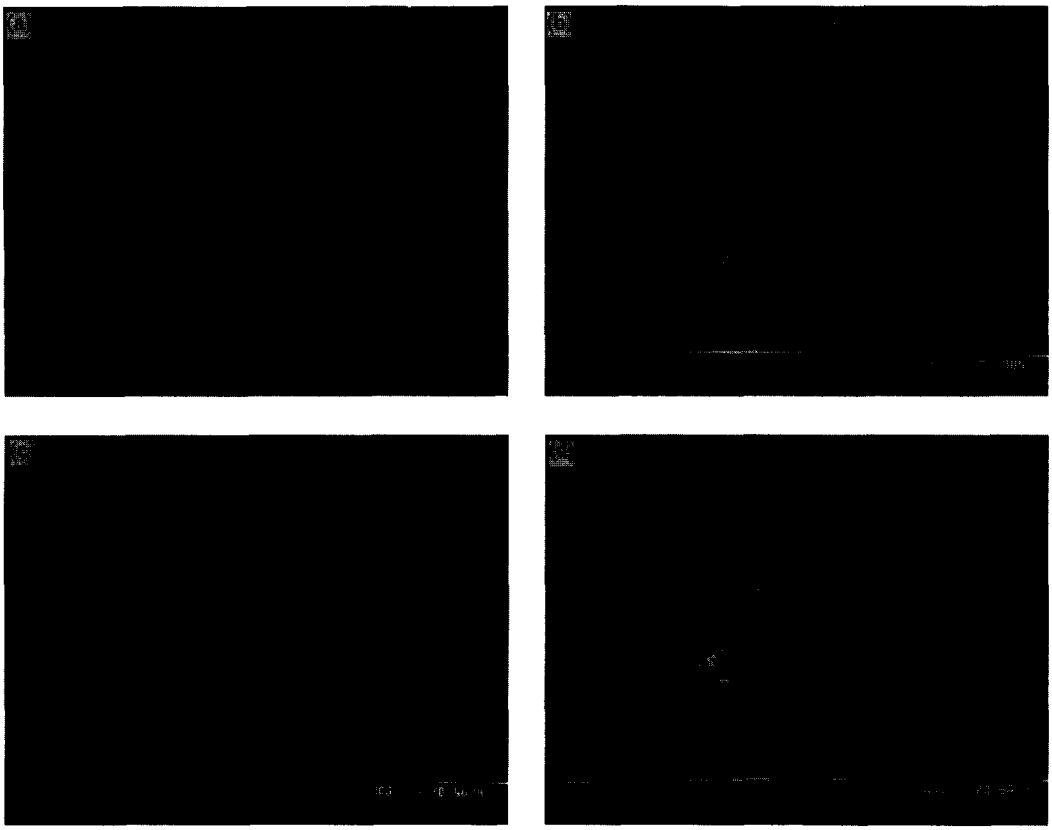

Fig. 8. Hollow and full grains: (a) hollow grain (acetone/water ratio < 0.055 kg acetone/kg water, experiment 16); (b) full grain (acetone/water ratio > 0.055 kg acetone/kg water, experiment 17); (c) enlargement of grain crusts presented in Fig. 6(a); (d) full grain (acetone/water ratio > 0.070 kg acetone/kg water, experiment 18).

increases for low water percentage, then decreases when the water proportion increases (see part A of this work [6]). If water enters into the droplet at constant temperature, the concentration of water decreases as the radius decreases. But, when the mass ratio of acetone/water is higher than 0.67 kg acetone/kg water + acetone mixture, the solubility of ketoprofen reaches a maximum for a value between 0.86 and 0.93 kg acetone/kg water + acetone mixture and the supersaturation cannot be reached only by water addition [5]. The temperature of the droplet must also be reduced for the creation of supersaturation. So, by combining the effect of temperature and water penetration, the profile of supersaturation ratio can be for example: $S^1 > S^2 > S^3$ and $S^3 < S^4$ and $S^4 > S^5 > S^6$ with $S^1 < S^6$. So with such a profile crystals can appear everywhere in the droplet.

The internal circulation homogenizes the concentration in the droplet.

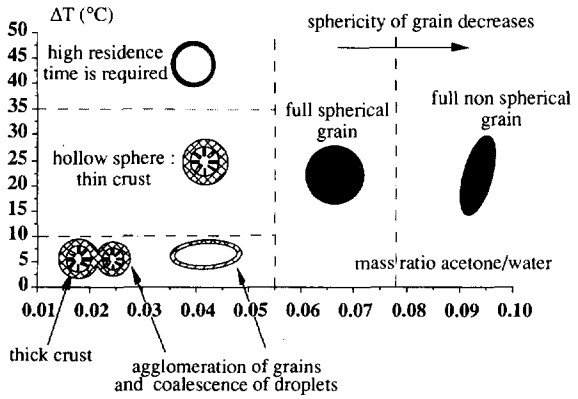

Fig. 9. Summary of different structures as function of ΔT and initial mass ratio of acetone/water.

6.3. Crystallization

The internal structures can be explained from the importance of the different phenomena.

6.3.1. Grains with a hole

These grains are formed from small droplets: the diameter of the droplet is lower than a critical diameter. The magnitude of the critical diameter can be calculated by modelling the transfer in the droplets [7].

6.3.1.1. Grains with one crust

When the difference of temperature between the organic phase and the aqueous phase is large (ΔT higher than 35 °C), one crust is formed by thermal effect. This crust then reduces the mass transfer of solvents. In this crust, the crystals have no preferential direction. This phenomenon is frequently encountered in the spray drying process.

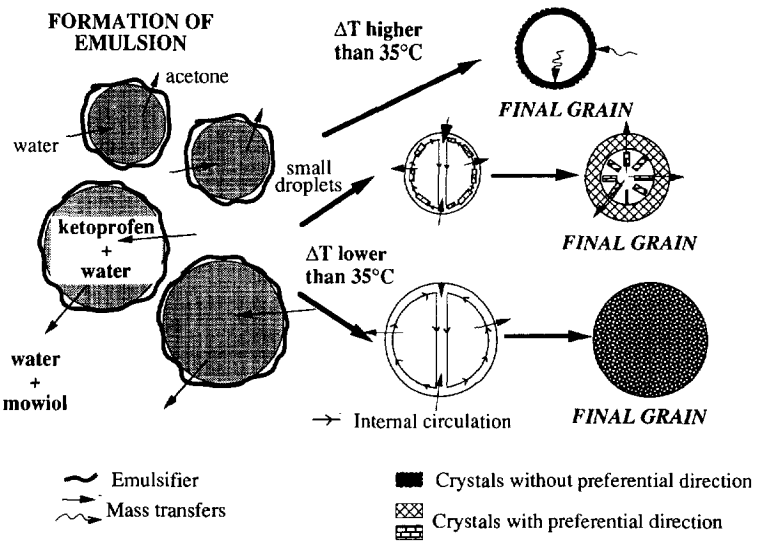

Fig. 10. Mechanism of grain formation by the quasi-emulsion process.

6.3.1.2. Grains with two crusts

When the difference of temperature is lower than 35 °C, most grains have a crust with two juxtaposed solid layers at their periphery. In that case, the mass transfer and the internal hydrodynamics are in competition.

Since the supersaturation limit is reached preferentially at the interface, the crystals appear at the surface of the grains. The liquid circulates in the droplet at rates higher than those produced by the mass transfer. These hydrodynamic movements allow the first crystals to grow. Since this circulation follows the periphery of the droplet, the growth of faces that are perpendicular to the movement is favoured [8]. The longest faces of crystals are perpendicular to the radius of the grain. These crystals form the first crust. When this crust becomes compact, internal circulation is reduced so only mass transfer continues through the first porous crust and the crystals grow in a direction parallel to the flux of transport or to the radius of the grain. These crystals form the second crust. They probably continue to grow during drying.

6.3.2. Full grains

Grains are formed from droplets with a diameter larger than the critical diameter. In that case, the internal liquid circulation created in the droplet is less important than that produced by the mass transfer. Since the rates of mass transfer are important, the induction time preceding the nucleation is very long (see part A of this work [6]). The internal circulation favours mixing in the liquid droplet. In these conditions, when nucleation occurs, the fine nuclei agglomerate to create a network of fine pores. In addition, ketoprofen presents a narrow metastable zone in the presence of crystals (part A of this work). Primary nucleation is then followed by secondary nucleation in the droplet. A full grain is then created after these two waves of nucleation.

7. Conclusion

This work gives an analysis of spherical crystallization experiments carried out in a batch laboratory scale device. The influences of operating parameters have been studied: difference of temperature; initial mass ratios of acetone/water, mowiol/water, and ketoprofen/acetone; organic solution flowrate; stirring rate, and capillary diameter. The analysis of these influences has permitted us to propose a mechanism of grain formation. This mechanism involves three steps: formation of droplets, creation of supersaturation by mass and heat transfer, and crystallization of ketoprofen in the droplets.

Three internal structures have been identified:

- internal structure with one crust
- internal structure with two crusts
- full internal structure.

The internal structure of grains depends on the initial size of droplets because this size governs the importance of phenomena occurring in the droplets. Modelling of grain formation has been published elsewhere [7].

Acknowledgements

The authors wish to acknowledge Rhône-Poulenc-Rorer Company and the French Ministère de l'Enseignement Supérieur et de la Recherche (MESR) for their financial support of this project.

Appendix A. Nomenclature

d	diameter (m)
dn_i	number percentage of particles

$(\bar{d}_n)_i$ mean number diameter in class i (m)
$(\bar{d}_v)_i$ mean volume diameter in class i (m)
D_p diameter of the propeller (m)
D_r diameter of the reactor (m)
m_0 initial mass with no tapping (g)
m_{500} initial mass after 500 tappings (g)
N rate of rotation (rpm)
Q_c flowrate ($m^3 s^{-1}$)
S supersaturation ratio (-)
T temperature (°C)
T_1 temperature of dissolution (°C)
T_2 initial temperature of water in crystallizer (°C)
w_a mass fraction of acetone in continuous phase (kg acetone/kg mixture)
w_k mass fraction of acetone in continuous phase (kg ketoprofen/kg mixture)
W_a mass ratio of acetone in water (kg acetone/kg water)
W_k mass ratio of ketoprofen in acetone (kg ketoprofen/kg acetone)
ΔT difference of initial temperatures between the dispersed and continuous phases (°C)
ρ_{app} apparent density ($g\ cm^{-3}$)
ρ'_{app} tapped apparent density ($g\ cm^{-3}$)
σ_d standard deviation (m)

References

[1] F. Espitalier, Ph.D. Thesis, INP Toulouse, France, 1994.
[2] A. Sano, T. Kuriki, Y. Kawashima, H. Takeuchi, T. Hino, T. Niwa, Chem. Pharm. Bull. 37 (8) (1989) 2183–2187.
[3] Y. Kawashima, in: D. Chulia, M. Deleuil, Y. Pourcelot, (Eds.), Powder Technology and Pharmaceutical Processes, Elsevier Science B.V., Amsterdam, The Netherlands, 1994, ch. 14, part 1, pp. 493–511.
[4] R. Clift, J.R. Grace, M.E. Weber, Bubbles, Drops and Particles, Academic Press, New York, 1978.
[5] F. Espitalier, B. Biscans, S. Peyrigain, C. Laguérie, Fluid Phase Equilibria 113 (1995) 151–171.
[6] F. Espitalier, B. Biscans, C. Laguérie, Chem. Eng. J. 68 (1997) 95–102.
[7] F. Espitalier, B. Biscans, J.R. Authelin, C. Laguérie, Trans. Inst. Chem. Eng. 75 A (1997) 257–267.
[8] C.Y. Tai, C.H. Lin, J. Crystal Growth 82 (1987) 377–384.